Time domain measurement of the THz refractivity of water vapor

Yihong Yang, Mahboubeh Mandehgar, and D. Grischkowsky*

School of Electrical and Computer Engineering, Oklahoma State University, Stillwater, OK 74078, USA
daniel.grischkowsky@okstate.edu

Abstract: We report the measurement of the essentially frequency independent refractivity of water vapor from 0.1 to 1 THz, independent of the simultaneous strong THz pulse broadening and absorption. The humidity dependent transit time of THz pulses through a 170 m long round trip path was measured to a precision of 0.1 ps, using a mode-locked laser as an optical clock.

OCIS codes: (250.0250) Optoelectronics; (320.7160) Ultrafast technology; (300.6495) Spectroscopy, terahertz; (010.1320) Atmospheric transmittance.

Reference and links

1. L. Essen, "The refractive indices of water vapour, air, oxygen, nitrogen, hydrogen, deuterium and helium," Proc. Phys. Soc. B **66**(3), 189–193 (1953).
2. L. Essen and K. D. Froome, "The refractive indices and dielectric constants of air and its principal constituents at 24,000 Mc/s," Proc. Phys. Soc. B **64**(10), 862–875 (1951).
3. K. D. Froome, "The refractive indices of water vapour, air, oxygen, nitrogen and argon at 72 kMc/s," Proc. Phys. Soc. B **68**(11), 833–835 (1955).
4. T. Manabe, Y. Furuhama, T. Ihara, S. Saito, H. Tanaka, and A. Ono, "Measurements of attenuation and refractive dispersion due to atmospheric water vapor at 80 and 240 GHz," Int. J. Infrared Millim. Waves **6**(4), 313–322 (1985).
5. C. C. Bradley and H. A. Gebbie, "Refractive index of nitrogen, water vapor, and their mixtures at submillimeter wavelengths," Appl. Opt. **10**(4), 755–758 (1971).
6. H. Matsumoto, "The refractive index of moist air in the 3-μm region," Metrologia **18**(2), 49–52 (1982).
7. R. J. Hill and R. S. Lawrence, "Refractive index of water vapor in the infrared windows," Infrared Phys. **26**(6), 371–376 (1986).
8. R. Schödel, A. Walkov, and A. Abou-Zeid, "High-accuracy determination of water vapor refractivity by length interferometry," Opt. Lett. **31**(13), 1979–1981 (2006).
9. D. Grischkowsky, S. Keiding, M. Exter, and C. Fattinger, "Far-infrared time-domain spectroscopy with terahz beams of dielectrics and semiconductors," J. Opt. Soc. Am. B: Opt. Phys.**7**(10), 2006–2015 (1990).
10. Y. Yang, A. Shutler, and D. Grischkowsky, "Measurement of the transmission of the atmosphere from 0.2 to 2 THz," Opt. Express **19**(9), 8830–8838 (2011).
11. Y. Yang, M. Mandehgar, and D. Grischkowsky, "Broad-band THz pulse transmission through the atmosphere," IEEE Trans. THz Sci. Technol. **1**, 264–273 (2011).
12. Y. Yang, M. Mandehgar, and D. Grischkowsky, "Understanding THz pulse transmission in the atmosphere," IEEE Trans. THz Sci. Technol. **2**, 406–415 (2012).
13. I. Wilke, A. M. MacLeod, W. A. Gillespie, G. Berden, G. M. H. Knippels, and A. F. G. van der Meer, "Single-shot electron-beam bunch length measurements," Phys. Rev. Lett. **88**(12), 124801 (2002).
14. A. M. Weiner, *Ultrafast Optics*, (John Wiley and Sons, Inc. 2009).
15. H. M. Pickett, R. L. Poynter, E. A. Cohen, M. L. Delitsky, J. C. Pearson, and H. S. P. Muller, "Sub-millimeter, millimeter, and microwave spectral line catalog," J. Quant. Spectrosc. Radiat. Transfer **60**(5), 883–890 (1998).
16. P. Debye, *Polar Molecules*, 89–90 (Dover Publ. Co., 1957).
17. B. R. Bean, and E. J. Dutton, *Radio Meteorology* (National Bureau of Standards, Monograph #92, March 1966), Chap. 1.
18. J. H. van-Vleck and V. F. Weisskopf, "On the shape of collision-broadened lines," Rev. Mod. Phys. **17**(2-3), 227–236 (1945).
19. C. H. Townes and A. L. Schawlow, *Microwave Spectroscopy* (Dover Publ. Co., 1975).
20. M. van Exter and D. Grischkowsky, "Optical and electronic properties of doped silicon from 0.1 to 2 THz," Appl. Phys. Lett. **56**(17), 1694–1696 (1990).
21. A. Deepak, T. D. Wilkerson, and L. H. Ruhnke, eds., *Atmospheric Water Vapor*, (Academic Press, 1980). This book is the Proceedings of the International Workshop on Atmospheric Water Vapor, Vail, Colorado, September 11–13, 1979.

#173948 - $15.00 USD Received 7 Aug 2012; revised 3 Oct 2012; accepted 30 Oct 2012; published 5 Nov 2012

22. D. E. Burch and D. A. Gryvnak, "Continuum absorption by water vapor in the infrared and millimeter regions," *Proceedings of the International Workshop on Atmospheric Water Vapor*, [21] 47–76 (1979).
23. Y. Scribano and C. Leforestier, "Contribution of water dimer absorption to the millimeter and far infrared atmospheric water continuum," J. Chem. Phys. **126**(23), 234301 (2007).

1. Introduction

The propagation of electromagnetic waves in the atmosphere is determined by the relatively small frequency-dependent part (of the order of 0.0003) of the index of refraction $n(\omega)$ and the absorption coefficient $\alpha(\omega)$. Because the frequency dependent part of the index is quite small, the refractivity term $[n(\omega) - 1]$ is usually discussed. The most variable component of the atmosphere is water vapor, which is responsible for the rapidly changing clouds, and the relative amount of water vapor can change in less than 1 hour. Even though water vapor is only one percent of the total atmosphere, at 50% relative humidity (RH) water vapor can account for more than 20% of the refractivity. The refractivity of water vapor is composed of two parts, a slowly-varying almost frequency-independent part, applicable from microwaves up to THz, into the infrared and the visible, and a strongly frequency-dependent part together with strong absorption in the water vapor rotational spectrum from 0.2 to 10 THz. Measurements of the refractivity of water vapor have been made at microwave [1,2], mm-wave [3,4], far-infrared (THz) [5], infrared [6,7], and optical frequencies [8]. Previously, until the results described here, all measurements of the refractivity of water vapor, determined the sum of both parts.

2. Experimental setup

Our direct measurement of the frequency-independent refractivity of water vapor ($n_o - 1$) involved measuring the transit time of THz pulses through a 170 m long round trip path to a precision of 0.1 ps, by using a mode-locked laser as an accurate optical clock. A 137 m round-trip sample chamber within the 170 m path allowed us to measure the transit time of the sharp leading edge of the reshaped THz pulses, as a function of the controllable humidity of the chamber. Our results are consistent with previous lower frequency microwave and mm measurements [1–3] and with two previous single frequency THz gas laser measurements of the total two-part refractivity [5].

For the long-path setup shown in Fig. 1, the THz pulses are generated and detected on photoconductive SOS chips by two 10mW, 800nm, laser beams of 80 fs pulses from a Ti-Sapphire Mode-locked laser with a 89.6948()() MHz repetition (clock) rate. The optical clock rate is measured to eight digits and is quite stable to six digits. Frequency drift and some jitter occurs in the last 2 digits, as indicated by the open brackets. By combining an optical train of large flat mirrors with a spherical 12 inch (30.5 cm) dia., 125 inch (317.5 cm) focal length telescope mirror coupled to the standard THz-TDS system [9], a 170 m round trip path for the propagating THz pulses was achieved [10–12].

In order to obtain the high S/N of the coherent sampling used in THz-TDS [9], the final propagation distance of 170.46 m was adjusted to be precisely equal to an integer number of round-trips (51 in this case) of the laser pulse in the mode-locked laser. Consequently, the delayed laser sampling pulses with pulse train number 52 were used to measure the THz pulses that have propagated 170.46 m. The sampling pulses are delayed by 51 pulses down the pulse train from the excitation pulses with number 1. As will be discussed below this approach is surprising stable, considering that the heavy mounts for the large mirrors M5-M9 are placed on the heavy concrete floor, and not on the optical table, and that the sampling pulses are 51 pulses down the laser pulse train from the excitation pulses.

#173948 - $15.00 USD Received 7 Aug 2012; revised 3 Oct 2012; accepted 30 Oct 2012; published 5 Nov 2012

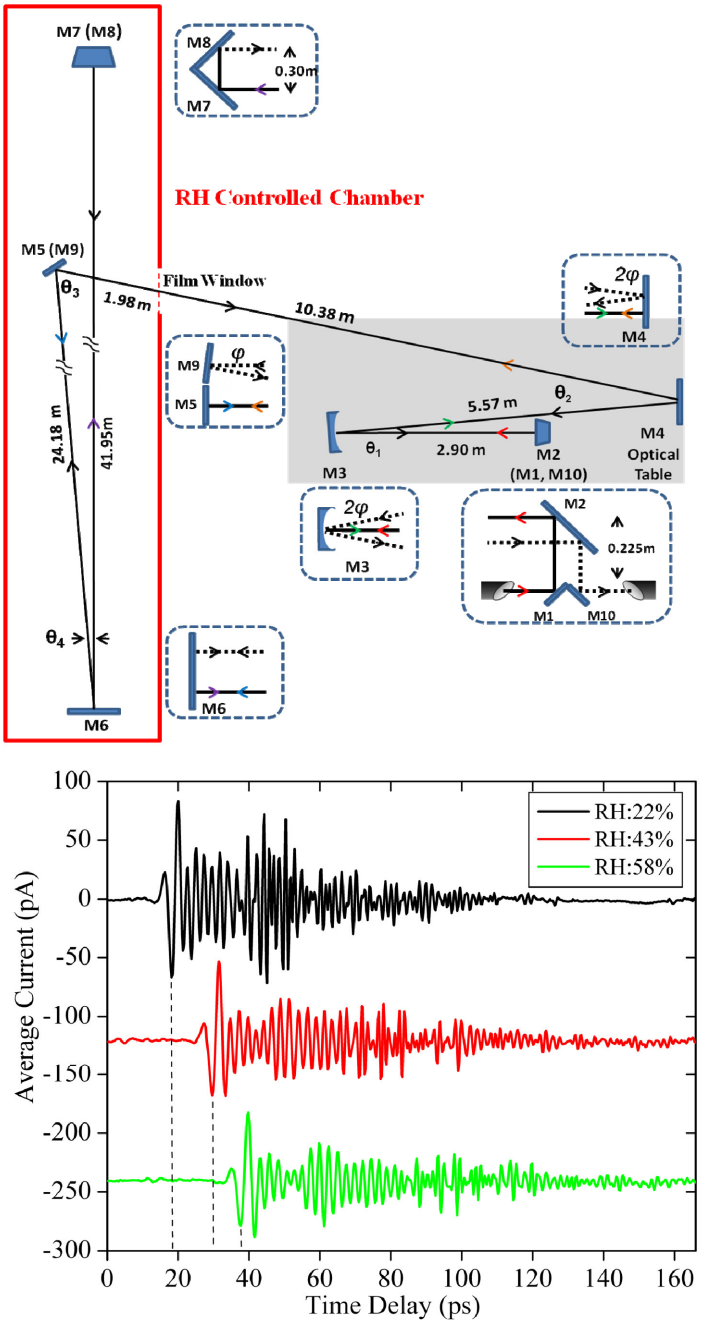

Fig. 1. Top (x-z plane) view of the long-path set-up with the sample chamber outlined (red online). Insets: Side (y-z plane) views of all mirrors. Solid lines show the optical path and the outgoing THz beam (in insets), dased lines show the incoming THz beam. Arrows indicate the THz beam direction, colors distinguish overlapping beams in the side view. The indicated angles are $\theta_1 = 5.4°$, $\theta_2 = 19°$, $\theta_3 = 80°$, $\theta_4 = 2.4°$, and $\varphi = -1.25°$. Three measured transmitted THz pulses (top) RH 22% (4.0 g/m^3), (middle) RH 43% (7.9 g/m^3), (bottom) RH 58% (10.6 g/m^3) at 21 °C show the frequency-independent water vapor delays with respect to the top pulse of $\Delta t = 11.5$ ps and $\Delta t = 19.5$ ps and, where $\Delta t = (n_o - 1)L/c$. The dashed lines mark the corresponding first minimums at 18.15 ps, 29.63 ps, and 37.63 ps.

#173948 - $15.00 USD Received 7 Aug 2012; revised 3 Oct 2012; accepted 30 Oct 2012; published 5 Nov 2012

This technique of matching path lengths by using the laser clock as a precise multiple-step delay line has previously been used to measure the pulse length of relativistic electron beam bunches [13]. Minimizing the temporal jitter in ultrafast laser systems is essential for such pump-probe spectroscopy of all types [14]. Usually, electronic systems coupled to laser sources are actively synchronized with precise feed-back control to periodic phenomenon. In contrast, our approach is completely passive, after we obtain the initial synchronization by adjusting the physical length of the long-path THz optical train.

The optical clock rate corresponds to a delay between pulses of 11.148918 ns, which is multiplied by 51 to give the total laser-clock defined path delay of 568.594835 ns. Over the course of an experiment, there are slow changes in the optical clock rate of the order of 100 Hz. If the clock rate is reduced by 100 Hz to 89.6947 MHz, the corresponding total time delay is increased to 568.595469 ns, causing a difference in the total long-path clock delay of 0.63 ps. This change in delay is accurately measured to 0.1 ps, and is almost equal to our observed drift of 0.6 ps/hour of the measured transmitted THz pulse [11]. The total drift is caused by both the laser-clock drift, which is easily measured by the frequency counter and by the slow drift of the length of the 170.46 m long THz optical train. A 149 m-long part of the 170.46 m optical train is directed by large mirrors on heavy mounts supported by the thick floating-slab concrete floor of the basement laboratory. The other 21.5 m-long part of the THz optical train is directed by mirrors supported on the stainless steel (SS) optical table.

We will now describe the optical train of our system in some detail from [11]. "The THz pulses are out-coupled vertically from the THz-TDS system by mirror M1, as shown in the Fig. 1 inset. The reflection from Mirror M2 initiates the elevated horizontal beam line (in the x-z plane) to the 32-cm (12.5 in) diameter, collimating mirror M3 with a focal length of 318 cm (125 in) and the corresponding radius of curvature of 635 cm (250) in). The focus of M3 is located at the confocal THz beam-waist of the THz-TDS system, for which the Gaussian beam-waist diameter is proportional to wavelength and is 10 mm at 1 THz. The reflected and collimated beam from M3 is directed to M4. The reflected THz beam from M4 is directed within the x-z plane to mirror M5, which, in turn, reflects the beam horizontally in the x-z plane to tall mirror M6. From M6, the beam is directed horizontally to M7. As shown in the inset, in order to spatially separate the returning and outgoing beam, mirror M7 reflects the beam vertically up 30.5 cm (12 in) to the upper mirror M8, which reflects the beam horizontally to tall mirror M6. Mirrors M7 and M8 form an air-spaced right angle prism. The center of the returning THz beam on mirror M6 is 30.5 cm above the center of the out-going THz beam on M6. The returning THz beam is reflected horizontally by M6 to the upper mirror M9 shown in the insert, which reflects the beam back to mirror M4 with a −1.25° (21.8 mrad) downward vertical tilt to optimize coupling to the THz receiver. The returning beam maintains the 1.25° vertical tilt after the reflection by M4 to the center of the focusing mirror M3. The focusing reflection of the returning beam by M3 also maintains the downward tilt and thereby directs the focus to M10 after the reflection by M2. The reflection from M10 removes the vertical tilt φ and directs the beam horizontally into the receiver.

We use large, optical-quality mirrors with Enhanced Aluminum coatings (which enhance the visible reflectivity for the initial alignment with a 15-mW HeNe laser. The large mirror sizes are: M4 is 40.6 cm x 40.6 cm (16-in x 16 in), M5 is 30.5 cm x 30.5 cm (12 in x 12 in); M6-M8 are 40.6 cm wide x 61 cm tall (16 in x 24 in), and M9 is 61 cm wide x 40.6 cm tall (24 in x 16 in)."

The massive concrete floor is considered to respond very slowly, on the order of many hours or days, to average temperature changes, while the temperature response of the SS table is much faster. It is important to note that stainless steel and concrete have approximately the same coefficient of thermal expansion 10^{-5} $(\Delta L/L)/\ ^{\circ}C$. Consequently, if the temperature difference ΔT between the concrete floor and the SS optical table remained the same, synchronization would be maintained, and the measured start time of the long-path transmitted THz pulse would not change with temperature. However, if the difference

#173948 - $15.00 USD Received 7 Aug 2012; revised 3 Oct 2012; accepted 30 Oct 2012; published 5 Nov 2012

temperature ΔT changed by 1 °C, a length difference of 170 m x 10^{-5}would occur, with the corresponding change in the start time of the THz pulse of 5.7 ps. This time change is approximately equal to the observed day to day and week to week changes.

The alignment of the long-path THz optical train typically requires no adjustments over periods as long as two-weeks. The main stability issue is the reproducibility of the THz input pulses to the optical train, caused by changes in the laser driving and sampling pulses.

As shown by the red box in Fig. 1, the entire 141.5 feet (43.1 m) long hallway in the THz laboratory is transformed into a humidity controlled sample chamber, by temporarily sealing the air-vents, lights, and lab-doors with plastic sheet and tape. The THz beam passes into and out of this chamber, through a 2.4 x 4.8 foot (73x146 cm^2), 12.5 μm thin plastic film window in the lab doorway. The total round trip path within the RH controlled chamber is 137 m. The humidity in the sample chamber can be increased and stabilized, by much as 30% from the ambient laboratory value, by 8 humidifiers and four 16 liter water heaters distributed uniformly along the hallway. The water heaters produce hot water for the humidifiers, while two large fans circulate the air during measurements. The chamber humidity is stabilized by an initial adjustment of the locations and humidifier settings of the humidifiers to obtain similar hygrometer readings throughout the chamber, and then letting the system run for approximately 30 minutes to reach a stable condition. Hygrometers, located at both ends of the chamber and on the optical table, measure RH and temperature.

3. Result and discussion

3.1 Experimental Measurements

In Fig. 1, the transmitted THz pulses for the dry reference (RH 22%), and the first wet sample (RH 43%) and the second wet sample (RH 58%) are shown. The sample pulses show arrival time delays of 11.5 ps and 19.5 ps, respectively compared to the reference pulse, due to the higher RH in the chamber. Based on the temperature and RH, the absolute water vapor

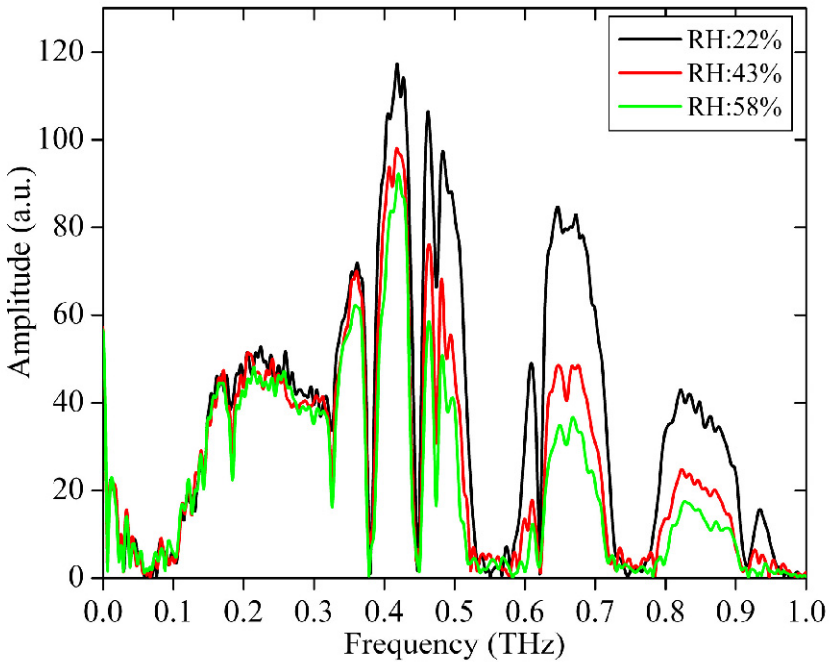

Fig. 2. Amplitude spectra of the transmitted pulses of Fig. 1.

#173948 - $15.00 USD Received 7 Aug 2012; revised 3 Oct 2012; accepted 30 Oct 2012; published 5 Nov 2012

density can be calculated to determine the corresponding frequency independent refractive index of water vapor. Moreover, the decaying higher-frequency chirped parts of the signal, occurring after the lower-frequency sharp leading edge of the pulses, are attenuated rapidly because of the increasing absorption with frequency, as shown in the corresponding amplitude spectra in Fig. 2.

The physical concepts, that the entire reshaped THz pulse is simply delayed by the frequency independent refractivity of water vapor and that the pulse reshaping is only determined by the strongly frequency-dependent part of the refractivity, have recently been experimentally and theoretically validated [12]. This work [12] showed the observed pulse reshaping to be in excellent agreement with the calculated reshaped pulse, using only the frequency dependent absorption $\alpha(\omega)$ and refractivity $n(\omega)$-1 obtained from the sum over all of the water vapor lines in the JPL database [15] up to 10 THz with the absorption and phase shifts of the van-Vleck Weisskopf theory, which has no frequency-independent refractivity.

The measurements (on different days) of the THz pulse time shifts, as a function of the changing RH are shown in Fig. 3(a). For this data the pulse delays at a specified RH change of the order of 5 ps from week to week because of the small changes in the long path delay with respect to the laser clock. Over the relatively short time of the measurement, this drift is negligible and consequently, all of the different curves have the same slope. The experimental data show the arrival time of first ascending zero crossing of the received THz pulses. The straight lines show a linear dependence on the chamber RH. These parallel lines (measured on different days) show the repeatability of the entire system and the chamber. From the actual delay, determined by extending the curves back to zero RH, we obtain our measured complete delay versus humidity curve shown in Fig. 3(b).

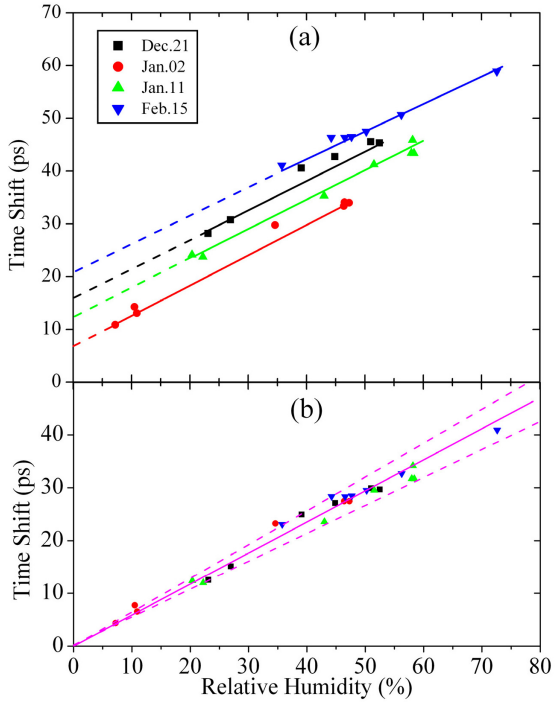

Fig. 3. (a) The measured pulse time-shift vs RH at 21 °C for four independent measurements, performed many weeks apart. (b) Replot of the data and extended lines of (a), with the time delay at zero RH subtracted from the data series. The overlap of all data was fit a straight line with a standard deviation of 1.40; and a slope: 5.84 ps/ RH 10%. For conversion to other units RH 54% at 21 °C is equivalent to 10.1 mm Hg and a water vapor density of 10 g/m^3.

#173948 - $15.00 USD Received 7 Aug 2012; revised 3 Oct 2012; accepted 30 Oct 2012; published 5 Nov 2012

Our Fisher 4083 hygrometers have an accuracy of ± RH 1.5%, independent of value of the reading. The temperature measurements are accurate to ± 0.4 °C. However, the uniformity of the humidity and temperature readings in the sample chamber vary by ± RH 3% for the humidity and ± 2 °C for the temperature. The time shift is measured to an accuracy of ± 0.1 ps, limited by the slow 0.6 ps/hour drift of the laser clock and the long-path length. The laboratory temperature and humidity are uniform, but they drift during a data run by typically RH 3% and 1 °C. This drift can be compensated theoretically. The RH 3% drift in the laboratory does change the optical delay of pulse 52, because the mode locked laser is in a dry-air enclosure, and is not affected by changes in laboratory humidity. All of this uncertainty is presented by the measurements in Fig. 3. All of the measurements presented in Fig. 3(b) are contained within the dashed curves with the slopes of 6.42 ps/RH 10% and 5.26 ps/RH 10%, where the best fitting curve has the slope of 5.84 ps/RH 10%.

The frequency-independent refractivity is determined from the relationship $\Delta t = (n_o - 1)L/c$, where L = 137 m and c is the free-space light speed. From this relationship and the measured slope of 5.84 ± 10% ps/RH 10% at 21 °C shown in Fig. 3(b), we obtain $(n_0 - 1) = 70 \times 10^{-6} \pm 10\%$ for the measured frequency-independent refractivity of water vapor at 21 °C and 10 g/m^3, over the frequency band from 0.10 THz to 0.95 THz.

The measured refractivity is 24% of the corresponding dry air value of 293 x 10^{-6} due to the atmospheric gases of nitrogen and oxygen. This dry air component remains constant during our measurements, which are only sensitive to the changing refractivity of water vapor. Our measurement of 70 ± 10% x 10^{-6} is consistent with 61 x 10^{-6} for the early 9.2, 24 and 72 GHz measurements at 20 °C and 10 mm Hg (9.9 g/m^3) [1–3]. A field, line-of-sight measurement over an open 810 m outdoor path measured the refractivity difference between two sources of 80 GHz and 240 GHz, by measuring the differential phase delay [4]. Compared to the above frequency independent value of 61 x 10^{-6} [1–3], the relatively small difference observed was between 1.15 x 10^{-6} and 1.25 x 10^{-6} for different daily temperatures with a water vapor density of 10 g/m^3 [4]. This measurement is consistent with a constant or slowing varying refractivity. Our measurement is also consistent with the previous total refractivity ($n(\omega) - 1$) single-frequency measurements of water vapor at 26 °C and 10 mm Hg (9.7 g/m^3) of 63 x 10^{-6} at 0.890 THz and 80 x 10^{-6} at 0.965 THz (using single line THz gas lasers) [5].

It is noteworthy that the water vapor refractivity drops by approximately 30 times when the frequency is increased to 30 THz (10 μm) and above. For example, the infrared measurements at 10.6 μm and 3.5 μm gave the refractivities (n–1) of 2.06 x 10^{-6} and 2.86 x 10^{-6}, respectively at 20 °C and 10 Torr (9.9 g/m^3) [7]. Another infrared measurement at 3.4 μm gave the refractivity of 2.87 x 10^{-6} at 20 °C and 10 mm Hg (9.9 g/m^3) [6]. Optical measurements over the range of 780 to 532 nm gave (n–1) of 2.3 x 10^{-6} at 20 °C with 1000 Pa (7.4 g/m^3) [8]; scaling this value to 1333 Pa (10 mm Hg) (9.9 g/m^3) gives (n-1) = 3.07 x 10^{-6}.

3.2 Microwave and mm-Wave Debye Theory approach

Previously, the low-frequency experimental results up to 100 GHz have been understood in terms of the Debye theory for a molecular vapor of permanent electric dipoles [16,17]. Initially, we will try to understand the very large change in $(n(\omega) - 1)$ for water vapor in the range between 1 and 30 THz, within the framework of Debye theory, as the non-resonant response of the dipole moments of the water molecules [16–19]. For low frequencies, the Debye theory dipole polarization of the vapor of water molecules will be in thermal equilibrium with an applied electric field with the frequency-dependent, complex Debye refractivity of [16–19],

$$\tilde{n}_D(\omega) - 1 = \left(\frac{2\pi N \mu^2}{3kT} \right) \Big/ \left(1 + i\,\omega\tau\right) \qquad (1)$$

#173948 - $15.00 USD Received 7 Aug 2012; revised 3 Oct 2012; accepted 30 Oct 2012; published 5 Nov 2012

where N is the number of molecules per cubic centimeter, μ is the permanent dipole moment of the water molecule, k is the Boltzmann constant, T is the absolute temperature, ω is the applied angular frequency and τ is the relaxation time required for the external field-induced orientations of the molecules to return to a random distribution after the field is removed. (Note, this mathematical dependence is the same as for Drude theory of electrical conductivity [20]). Equation (1) can be rewritten in the form below to enable simple comparison with the measurements

$$\tilde{n}_D(\omega) - 1 = \frac{n_0(0) - 1}{1 + i\,\omega\tau} \tag{2}$$

where $(n_o(0) - 1)$ is the Debye refractivity at zero frequency. The Debye refractivity can be rewritten in terms of the real and imaginary parts as

$$\tilde{n}_D(\omega) - 1 = \frac{n_0(0) - 1}{1 + (\omega\tau)^2} - i \cdot \frac{[n_0(0) - 1] \cdot \omega\tau}{1 + (\omega\tau)^2} \tag{3}$$

Initially, we are concerned with the real part of the Debye refractivity $(n_o(0) - 1)/ [1 + (\omega\tau)^2]$, which falls off from the zero frequency as a Lorentzian with the half-width of $\omega_{1/2}\,\tau = 1$, equivalent to $f_{1/2} = 1/(2\pi\tau)$, where f is frequency. Note that there are only two parameters in the theory, $(n_o(0) - 1)$ and τ; $(n_o(0) - 1)$ can be directly calculated from Eq. (1) as,

$$n_0(0) - 1 = \frac{2\pi N \mu^2}{3kT} \tag{4}$$

using the following parameters; water vapor density of 10 g/cm^3 at 20 °C (T = 293 K), corresponding to N = 3.34 x 10 ^{17}/cm^3 ; μ = 1.85 Debye = 2.07 x 10^{-18} StatC-cm; and k = 1.38 x 10^{-16} [g (cm/s)^2]. Evaluation of Eq. (4) with the above parameters gives the value of n_o (0) – 1 = 65 x 10^{-6}, in good agreement with previous low-frequency measurements [1–3] with n_o (0) – 1 = 61 x 10^{-6}

In order to explain the experimental results discussed above, where the real part of Debye refractivity changes from 70 x 10^{-6} at zero frequency to much less than 2 x 10^{-6} at 30 THz, which is considered to be due to other physical processes, and remains essentially constant all the way to optical frequencies. The lower frequency Debye response is considered to be defined by the frequency half-width of $f_{1/2}$ = 2.0 THz. This assumption gives a monotonically decreasing refractivity from 70 x 10^{-6} at zero frequency to 0.8 x 70 x 10^{-6} at 1.0 THz, which is consistent with the previous measurements [1–8], and the previous Debye theory approach [16,17]. However, this value of $f_{1/2}$ = 2.0 THz is exceptionally large compared to the collision frequency of 3.5 GHz [12] for the water rotational lines at similar conditions of atmospheric pressure, water vapor density and temperature.

Similarly, the Debye power absorption coefficient is obtained from the product of 2ω/c and the imaginary part of the Debye refractivity [16–19],

$$\alpha_D(\omega) = 2\left(\frac{\omega}{c}\right) \cdot \frac{[n_0(0) - 1] \cdot \omega\tau}{1 + (\omega\tau)^2} \tag{5}$$

As shown in Ref. 12, the calculated amplitude transmission determined by α(ω) for the resonant lines was in good agreement with observations. Consequently, the Debye broad-band absorption over this same range must be smaller than the observed water vapor continuum absorption [21,22], in order to provide a self-consistent understanding of the previous measurements. For our conditions of $(n_o(0) - 1)$ = 70 x 10^{-6}, and with $f_{1/2}$ = 2.0 THz, at 1 THz we obtain $\alpha(\omega)_D$ = 1.17/m equivalent to 5.1 dB/m = 5100 dB/km, which is impossibly large compared to our experiments with longer paths [12], and with respect to the

#173948 - $15.00 USD Received 7 Aug 2012; revised 3 Oct 2012; accepted 30 Oct 2012; published 5 Nov 2012

long-standing atmospheric absorption curves, Figs. 1 and 2 of [10]. With respect to the continuum curve on Fig. 1 [10], the calculated $\alpha(\omega)_D$ is approximately 230 times too large at 1 THz and 190 times too large at 0.3 THz.

It is important to note, that the unusual absorption lineshape $\alpha(\omega)_D$ of the Debye response starts at zero, at zero frequency and initially increases quadratically with frequency, but when $\omega\tau$ becomes greater than 1, monotonically approaches the constant high-frequency limit α_D(limit), given below

$$\alpha_D\left(limit\right) = 2\frac{n_0\left(0\right)-1}{\left(c\tau\right)} \tag{6}$$

For our example, $1/\tau = 2\pi$ x 2 THz, the α_D(limit) = 5.86/m = 25.4 dB/m which is equivalent to 25,400 dB/km and is many orders of magnitude higher than experiment.

These impossibly large values show the previous opinion for measurements up to 100 GHz [17], that the Debye response of the vapor of permanent electric dipoles was the cause of the refractive delay, is physically incorrect. Thus, there must be other causes of this delay, such as water dimers, and perhaps clusters [21–23]. However, the effects of dimers and clusters would be expected to increase as the molecular number density squared, and our measurements show a linear dependence. Another possibility would be that the far wings of the resonance lines are broader than predicted.

3.3 Relationship of van-Vleck Weisskopf theory to Debye theory

The van-Vleck Weisskopf resonant lineshape theory has been shown to converge to the Debye theory as the resonant frequency approaches zero [18,19]. This broadened view of the dielectric response of water vapor connects this work of measurements of THz pulse delay with our previous work of measurements and theoretically fitting THz pulse reshaping [12]. There, the excellent reshaping fit was obtained by accurate calculations of the frequency dependent refractivity and absorption coefficients obtained by a sum over all the water lines (1305 lines) in the JPL database [15] from the first line at 22.3 GHz up to 10 THz [12]. The real part of the refractivity $(n(\omega) - 1)$ obtained from Eqs. (2) and (3) of [12] is mathematically expected to converge to the above Eq. (1) for very low frequencies with respect to the 7 GHz FWHM linewidth of the resonance lines [18,19], producing a narrow Lorentzian peak at zero frequency with an amplitude given by Eq. (4), and with a half width of 3.5 GHz. This subtle mathematical prediction is not shown in our numerical calculations of Eqs. (2) and (3) of [12], for which $(n(\omega) - 1)$ approaches zero to within closer than 0.1 x 10^{-7}, as the frequency approaches zero to within 0.2 GHz, as shown in Fig. 3(b) [12]. Another possibility to explain the large frequency-independent refractivity is that if the far wings of the resonance lines would be broader than predicted by v-VW theory. It is to be noted that for a test, we have doubled and quadrupled the v-VW linewidth of 7 GHz [12] and for both linewidths, 14 GHz and 28 GHz the calculated $(n(0) - 1)$ was unchanged by less than 0.1 x 10^{-7} .

Consequently, the total refractivity of water vapor from 1 GHz to 2 THz can be considered to be sum of that of a water vapor component with a Debye-like refractivity and the corresponding sum $(n(\omega) - 1)$ from all of the water lines given by Eqs. (2) and (3) of [12], as shown below in Eq. (7) and the corresponding Fig. 4,

$$n_{H_2O}\left(\omega\right)-1=\frac{n_0\left(0\right)-1}{1+\left(\omega\tau\right)^2}+\left[n\left(\omega\right)-1\right] \tag{7}$$

#173948 - $15.00 USD Received 7 Aug 2012; revised 3 Oct 2012; accepted 30 Oct 2012; published 5 Nov 2012

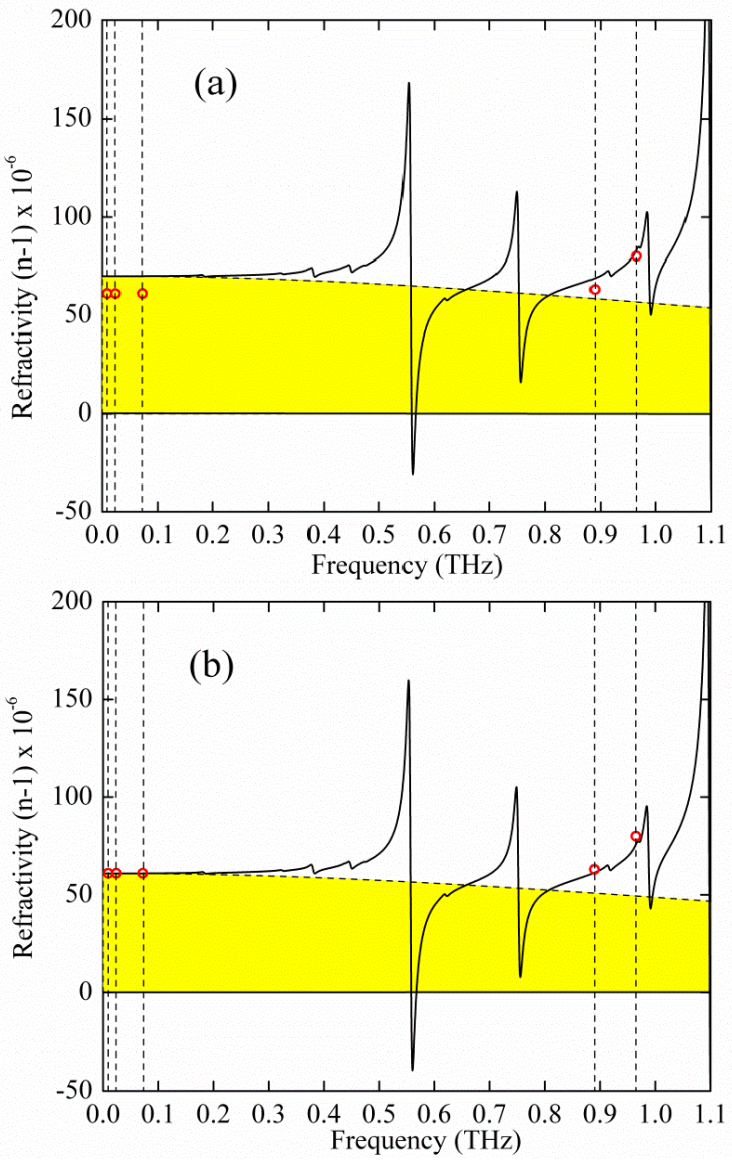

Fig. 4. Total refractivity of water vapor at 20 °C and 10 g/m^3. (a). The calculated refractivity of all the water vapor lines (Fig. 3(b) [12]), added to the measured frequency-independent refractivity (yellow highlight) of (70 x 10^{-6})/[1 + (f/$f_{1/2}$)^2] for $f_{1/2}$ = 2 THz. (b) The calculated refractivity of all the water vapor lines [12], added to the adjusted frequency-independent refractivity (yellow highlight) of (61 x 10^{-6})/[1 + (f/$f_{1/2}$)^2] for $f_{1/2}$ = 2 THz. The measurements of [1–3] are indicated by the three open circles at 61 x 10^{-6} on the dashed lines at 9.2, 24 and 72 GHz, respectively. The measurements of [5] are indicated by the two open circles at 63 and 80 x 10^{-6} on the dashed lines at 0.890 and 0.965 THz. It should be noted that without the frequency-independent term (n(0) – 1)/[1 + (f/$f_{1/2}$)^2], the curves drop to the zero base line, and become identical to Fig. 3(b) [12].

However, given the uncertainty of the water vapor component, the relationship for total absorption coefficient is not known, and for now will be simply considered to be given by the sum $\alpha(\omega)$ from all of the water lines given by Eq. (1) of [12].

#173948 - $15.00 USD Received 7 Aug 2012; revised 3 Oct 2012; accepted 30 Oct 2012; published 5 Nov 2012

Figure 4 shows the total refractivity of water vapor, which is the sum of the calculated refractivity from all of the resonance lines (Fig. 3(b) of [12]) and the frequency–independent refractivity multiplied by the Debye Lorentzian fall-off term, $(n(0) - 1)/[1 + (f/f_{1/2})^2]$ with $f_{1/2}$ = 2 THz. Figure 4(a) shows our measurement of $(n(0) - 1) = 70 \times 10^{-6}$, which links together all of the previous measurements [1–8]. Measurements [1–3, 5] are shown in Fig. 4. By reducing 70×10^{-6} to 61×10^{-6} in order to fit the 3 low frequency measurements [1–3], while keeping the same Debye fall-off, the excellent agreement shown in Fig. 4(b) is obtained. This good agreement is also consistent with the measured refractivity difference between 80 GHz and 240 GHz of only $1.2 \pm 0.5 \times 10^{-6}$ [4]. The agreement in Fig. 4(b) strongly supports our interpretation, provides a measure of the Debye fall-off, and shows the importance of the identification of the water vapor component responsible for the Debye-like response.

4. Summary

We have demonstrated that it is possible to make coherent optoelectronic THz pulse transmission measurements over a very long 170.46 m path, by using the mode-locked driving laser as an optical clock. For this technique with respect to the optical pumping (number 1)

pulses, the sampling pulses are from delayed pulse number n + 1 on the output pulse train, whereby the total transit time through the long path sample is equal to n cycle times of the laser. This gives a measurement accuracy of 0.1 ps over a delay time of more than 568.59 ns, for which n = 51 cycles.

Using this new capability, the essentially frequency-independent refractivity of water vapor was measured to be $(n_0 - 1) = 70 \times 10^{-6} \pm 10\%$ from 0.1 to 0.95 THz. This result is consistent with earlier measurements and is the first time-domain and consequent frequency band measurement, that is independent of the frequency dependence of the strong water rotational lines. The magnitude is exceptionally large, and is comparable to the changes caused by the absorption lines of water vapor. Further measurements are planned with better stabilization of the sample chamber to significantly improve our accuracy. In addition, we plan to extend the measurements to higher frequency.

The previous Debye theory approach [16,17] using the permanent dipole moments of the water molecules gives good agreement with measurements of the refractivity from 1 GHz to 1 THz with the slowly varying refractivity $(n(0) - 1)/[1 + (f/f_{1/2})^2]$ with $f_{1/2}$ = 2 THz. However, for water vapor $f_{1/2}$ = 3.5 GHz [12], and the corresponding absorption from the Debye theory with $f_{1/2}$ = 2 THz is impossibly high. Consequently, the component of water vapor responsible for the slowly varying refractivity is unknown. This component could perhaps be water dimers, trimers or clusters, but the expected number density squared effect was not observed. Another possibility to explain the observed refractivity is that if the far wings of the water resonance lines would be much broader than predicted by v-VW theory.

Acknowledgments

This work was partially supported by the DTRA (10-2960M), and the National Science Foundation. We acknowledge helpful readings of this manuscript by Joseph S. Melinger.

#173948 - $15.00 USD Received 7 Aug 2012; revised 3 Oct 2012; accepted 30 Oct 2012; published 5 Nov 2012